

Ram pressure stripping the hot gaseous halos of galaxies in groups and clusters

I. G. McCarthy^{1*}, C. S. Frenk¹, A. S. Font¹, C. G. Lacey¹, R. G. Bower¹,
N. L. Mitchell¹, M. L. Balogh² and T. Theuns^{1,3}

¹*Department of Physics, University of Durham, South Road, Durham, DH1 3LE*

²*Department of Physics and Astronomy, University of Waterloo, Waterloo, ON, N2L 3G1, Canada*

³*Department of Physics, University of Antwerp, Campus Groenenborger, Groenenborgerlaan 171, B-2020 Antwerp, Belgium*

Accepted XXXX. Received XXXX; in original form XXXX

ABSTRACT

We use a large suite of carefully controlled full hydrodynamic simulations to study the ram pressure stripping of the hot gaseous halos of galaxies as they fall into massive groups and clusters. The sensitivity of the results to the orbit, total galaxy mass, and galaxy structural properties is explored. For typical structural and orbital parameters, we find that $\sim 30\%$ of the initial hot galactic halo gas can remain in place after 10 Gyr. We propose a physically simple analytic model that describes the stripping seen in the simulations remarkably well. The model is analogous to the original formulation of Gunn & Gott (1972), except that it is appropriate for the case of a spherical (hot) gas distribution (as opposed to a face-on cold disk) and takes into account that stripping is not instantaneous but occurs on a characteristic timescale. The model reproduces the results of the simulations to within $\approx 10\%$ at almost all times for all the orbits, mass ratios, and galaxy structural properties we have explored. The one exception involves unlikely systems where the orbit of the galaxy is highly non-radial and its mass exceeds about 10% of the group or cluster into which it is falling (in which case the model under-predicts the stripping following pericentric passage). The proposed model has several interesting applications, including modelling the ram pressure stripping of both observed and cosmologically-simulated galaxies and as a way to improve current semi-analytic models of galaxy formation. One immediate consequence is that the colours and morphologies of satellite galaxies in groups and clusters will differ significantly from those predicted with the standard assumption of complete stripping of the hot coronae.

Key words: hydrodynamics — methods: N-body simulations — galaxies: clusters: general — galaxies: evolution — galaxies: structure — cosmology: theory

1 INTRODUCTION

There are marked differences in the observed properties of the field and cluster galaxy populations. Perhaps the best known difference is the larger fraction of galaxies that are ellipticals or S0s (and the correspondingly lower spiral fraction) in clusters relative to the field (e.g., Dressler 1980; Goto et al. 2003). Not only are the morphologies of cluster galaxies different from those of field galaxies, but so too are a variety of their other observed properties, including colours (e.g., Balogh et al. 2004; Hogg et al. 2004), star forming properties (e.g., Poggianti et al. 1999; Balogh et al. 2000; Gomez

et al. 2003), and the distribution and total mass of their gaseous component (e.g., Cayatte et al. 1994; Solanes et al. 2001). These observed differences indicate that the dense environments of groups and clusters are somehow strongly modifying the properties of galaxies as they fall in.

Uncovering the physical mechanisms that give rise to the observed variation in galaxy properties has been an active topic of research over the past two or three decades (e.g., Dressler 1984; Sarazin 1988). One of the most commonly mentioned processes is ram pressure stripping (Gunn & Gott 1972). Here the gaseous component (which can be composed of both cold atomic/molecular gas and a hot extended component) of the orbiting galaxy is subjected to a wind due to its motion relative to the intracluster medium

* E-mail: i.g.mccarthy@durham.ac.uk (IGM)

(ICM). The gas will be stripped if the wind is sufficiently strong to overcome the gravity of the galaxy. Recently, direct observational evidence for the ram pressure stripping of galaxies in clusters has been provided by long (up to tens of kpc) tails of gas seen to be trailing behind several cluster galaxies (e.g., Sakelliou et al. 2005; Crowl et al. 2005; Vollmer et al. 2005; Sun & Vikhlinin 2005; Machacek et al. 2006; Sun et al. 2007a). Such stripping could at least partially account for the differing properties of cluster and field galaxies.

There have been numerous theoretical studies dedicated to calculating the effects of ram pressure stripping on galaxies using hydrodynamic simulations or semi-analytic models. The vast majority of these studies have focused on the stripping of cold gaseous disks with an emphasis on whether this can account for the observed lower star formation rates (and redder colours) of cluster spirals relative to their field counterparts (e.g., Abadi et al. 1999; Quilis et al. 2000; Vollmer et al. 2001; Okamoto & Nagashima 2003; Mayer et al. 2006; Roediger et al. 2006; Hester 2006; Jachym et al. 2007; Roediger & Brüggen 2006; 2007). However, the stripping of extended *hot* gaseous halos of galaxies is only just beginning to be explored (e.g., Kawata & Mulchaey 2007) and has not yet been studied in a detailed and systematic way. The hot extended component is predicted to exist around most massive galaxies by semi-analytic models and cosmological simulations and is directly observable at X-ray wavelengths in the case of normal ellipticals. If the hot gaseous halo is completely stripped (as is typically assumed), the only fuel available for star formation is that which resided in the cold component when the galaxy first fell into the cluster. (This process of removing the supply of halo gas is sometimes referred to as “strangulation” or “starvation”.) However, if the hot halo remains intact for some time it can, via radiative cooling losses, replenish the cold component and potentially significantly prolong star formation. This, in turn, would affect the colours and morphologies of cluster galaxies (e.g., Larson et al. 1980; Abadi et al. 1999; Benson et al. 2000; Balogh et al. 2000).

Aspects of the stripping of the *hot* gaseous halos of galaxies in clusters have been considered in previous work (e.g., Gisler 1976; Sarazin 1979; Takeda et al. 1984). Mori & Burkert (2000) studied the stripping of dwarf galaxies subject to a constant wind using two-dimensional simulations and found that the relatively shallow potential wells of these systems cannot retain their hot gas component for long. However, these authors did not study more massive systems, such as normal ellipticals and spirals, where stripping of the hot ($\gtrsim 10^6$ K) halo should be much less efficient due to their higher masses and deeper potential wells. [Indeed, a recent X-ray survey of massive galaxies in hot clusters by Sun et al. (2007b) has revealed that *most* of the galaxies have detectable hot gaseous halos.] A few other studies have examined the stripping of more massive systems but not in the context described above. In particular, they have largely focused on the metal enrichment of the ICM (e.g., Schindler et al. 2005; Kapferer et al. 2007), the X-ray properties of the galaxies (Toniazzi & Schindler 2001; Acreman et al. 2003) or the generation of “cold fronts” (e.g., Takizawa 2005; Ascasibar & Markevitch 2006).

In the present paper, we carry out a detailed study of the ram pressure stripping of the hot gaseous halos of galax-

ies as they fall into groups and clusters. This is performed using a large suite of controlled hydrodynamic simulations. Unlike most previous studies, we use full three-dimensional (3D) simulations in which the galaxies fall into a massive “live” group or cluster on realistic orbits. One important aim is to derive a physically simple and accurate description of the stripping seen in the simulations that can be easily employed in the modelling of observed or cosmologically-simulated galaxies. An additional motivation for deriving such a model is to improve the treatment of ram pressure stripping in semi-analytic models of galaxy formation. At present, these models typically assume that the hot gaseous halos of galaxies are stripped at the instant they cross the virial radius of the group or cluster. Clearly, this is not a realistic assumption, especially in the case where the mass of the galaxy is not negligible compared to that of the group or cluster. Such semi-analytic models tend to predict group and cluster galaxies whose colours are too red compared to observations (e.g., Weinmann et al. 2006; Baldry et al. 2006). If the ram pressure stripping of the hot gaseous halos of cluster galaxies is not as (maximally) efficient as assumed by these models, the resulting galaxies would be bluer and perhaps in better agreement with observations.

The present paper is structured as follows. In §2, we present a discussion of our simulation setup and the results of convergence tests that demonstrate the robustness of our findings. In §3, we first outline a simple analytic model for ram pressure stripping that is based on the original formulation of Gun & Gott (1972) but which is appropriate for spherically-symmetrical gas distributions (as opposed to disks). We then compare this model to a wide variety of simulations and demonstrate that it provides an excellent match to the mass loss seen in the simulations. Finally, in §4, we summarise and discuss our findings.

2 SIMULATIONS

To study the ram pressure stripping of galaxies orbiting in massive groups and clusters, we make use of the public version of the parallel TreeSPH code GADGET-2 (Springel 2005). By default, this code implements the entropy-conserving SPH scheme of Springel & Hernquist (2002). The procedure we use to set up our simulations is quite similar to that described in McCarthy et al. (2007a) (hereafter, M07). We outline the basic procedure and note any relevant differences between our setup and that of M07.

In this study, ram pressure stripping is explored in two types of simulations. We refer to the first type as the “uniform medium” runs, where a galaxy is run through a uniform gaseous medium at constant velocity. In the second type of simulations (the “2-system” runs), the galaxies are placed on realistic orbits through a massive “live” galaxy group. In the uniform medium runs, the ram pressure to which the galaxy is exposed is effectively constant with time. Furthermore, there is no external gravitational potential (i.e., due to a massive group or cluster) to tidally distort or strip the galaxy. As a result, these simulations should provide a pure test of ram pressure stripping and should be easier to model than the second type of simulations. On the other hand, if the lessons learnt from modelling the uniform medium runs do not also generally apply to more realistic situations, such

as those in the 2-system runs, they will be of little practical use. This is why we have elected to use both types of simulations to study this problem.

2.1 Initial conditions and simulation characteristics

The galaxies (and the groups into which they fall, in the case of the 2-system runs) are represented by spherically-symmetric systems composed of a realistic mixture of dark matter and diffuse baryons.

The dark matter is assumed to follow the NFW distribution (Navarro et al. 1996; 1997):

$$\rho(r) = \frac{\rho_s}{(r/r_s)(1 + r/r_s)^2} \quad (1)$$

where $\rho_s = M_s/(4\pi r_s^3)$ and

$$M_s = \frac{M_{200}}{\ln(1 + r_{200}/r_s) - (r_{200}/r_s)/(1 + r_{200}/r_s)} \quad (2)$$

Here, r_{200} is the radius within which the mean density is 200 times the critical density, ρ_{crit} , and $M_{200} \equiv M(r_{200}) = (4/3)\pi r_{200}^3 \times 200\rho_{\text{crit}}$.

The only ‘free’ parameter of the NFW profile is the scale radius, r_s . The scale radius is often expressed in terms of a concentration parameter, $c_{200} \equiv r_{200}/r_s$. By default, we adopt the mean mass-concentration ($M_{200} - c_{200}$) relation derived from the *Millennium Simulation* (Springel et al. 2005) by Neto et al. (2007). This relationship is similar to that derived previously by Eke et al. (2001).

For simplicity, the diffuse baryons are assumed to initially trace the dark matter distribution, with the ratio of gas to total mass set to the universal ratio $f_b = \Omega_b/\Omega_m = 0.022h^{-2}/0.3 = 0.141$, where h is the Hubble constant in units of $100 \text{ km s}^{-1} \text{ Mpc}^{-1}$. The other properties of the diffuse gas (i.e., temperature and pressure profiles) are fixed by ensuring the gas is initially gravitationally bound and in hydrostatic equilibrium,

$$\frac{dP(r)}{dr} = -\frac{GM(r)}{r^2} \rho_{\text{gas}}(r) \quad (3)$$

While the assumption that the gas initially traces the dark matter is reasonable for the bulk of the baryons in massive groups and clusters (e.g., Vikhlinin et al. 2006; McCarthy et al. 2007b), it is almost certainly not a very realistic approximation for relatively low-mass systems, such as galaxies. The reason, of course, is that non-gravitational physics, such as cooling and feedback due, for example, to supernovae and/or AGN, which are neglected in our simulations, can significantly alter the properties of the gas in these systems. These processes are poorly understood and the properties of the gas will likely depend sensitively on the assumed feedback model. Therefore, any distribution we select for the hot gaseous halo of the galaxies will be somewhat *ad hoc*. The important point, however, is that one can use the simulations to develop a *physical* model for ram pressure stripping that can, with some confidence, be applied more generally. We argue that the analytic model developed below is just such a model. As will be demonstrated, tuning the model to match just one of our simulations results in very good agreement with all the other simulations, in spite of their widely varying physical conditions.

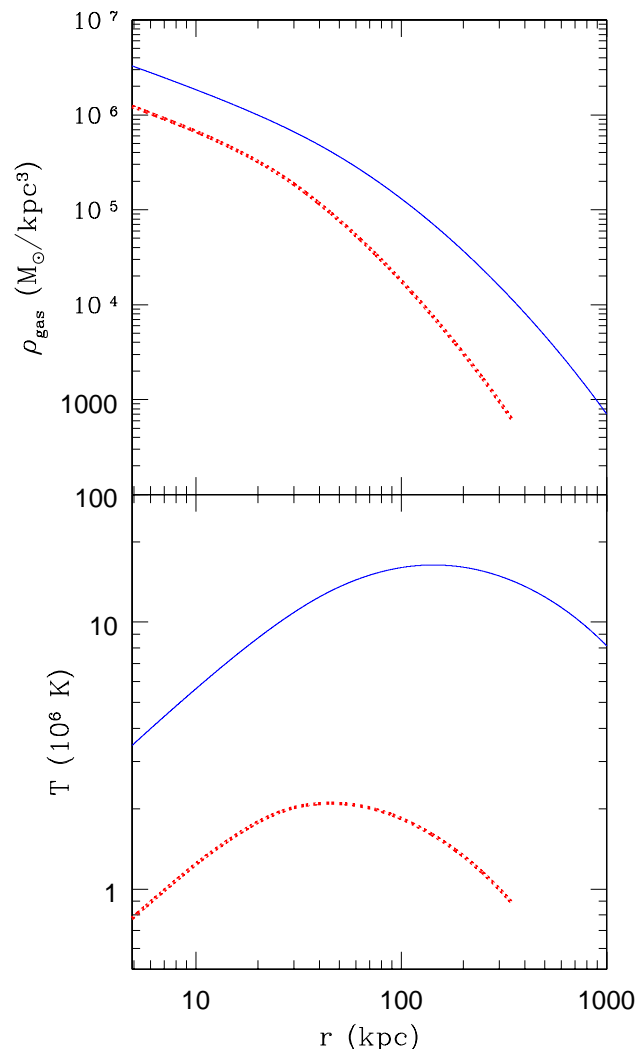


Figure 1. The initial gas density (top) and temperature (bottom) profiles for the hot halo of a galaxy with mass $M_{200} = 4 \times 10^{12} M_{\odot}$ (dotted red curves) and a group with mass $M_{200} = 10^{14} M_{\odot}$ (solid blue curves).

The reader is referred to §2 of M07 for a detailed discussion of how we establish equilibrium configurations of dark matter and gas particles that follow an NFW distribution¹. In the case of the 2-system runs, the more massive system is set to have a total mass of $M_{200} = 10^{14} M_{\odot}$, while the less massive systems have masses in the range $2 \times 10^{12} M_{\odot} \leq M_{200} \leq 10^{13} M_{\odot}$ (i.e., mass ratios from 50:1 to 10:1). Thus, the 2-system runs represent galaxies

¹ However, one difference of note is that instead of using the dark matter particle positions from our isolated runs to set the positions of the gas particles, we now morph a glass distribution into the desired NFW profile to set the gas particle positions (see §2 of M07). This was done to ensure a perfectly ‘cold’ start. We have run our galaxies and groups (with both baryons and dark matter particles in place) in isolation for many dynamical times and verified that they are stable, unevolving systems.

with masses comparable to or larger than a normal elliptical falling into a moderate mass group/low mass cluster. Note that for galaxies within this mass range, the mean temperature of their gaseous halos ranges between $\approx 1 - 3 \times 10^6$ K. In Fig. 1, we show the initial gas density and temperature profiles for the hot gaseous halo of one of the galaxies and for the ICM of the $10^{14} M_\odot$ group.

The default gas particle mass, m_{gas} , is set to $2 \times 10^8 f_b M_\odot$, while the default dark matter particle mass, m_{dm} , is set to $2 \times 10^8 (1 - f_b) M_\odot$. In the 2-system runs, these masses are fixed for both the group and the galaxy. This implies that the group is resolved with half a million gas and dark matter particles (each) within r_{200} . The gravitational softening length for both the gas and dark matter particles is set to 5 kpc for all our simulations. (We have experimented with different values of this parameter and find no significant differences in the results.)

A standard set of SPH parameters is adopted (e.g., Springel 2005). The number of SPH smoothing neighbour particles is set to 32, the artificial viscosity α_{visc} parameter is set to 0.8 (see §2.2), and the Courant timescale coefficient is set to 0.1.

The simulation data are output frequently, at intervals of 50 Myr, and the simulations are run for a maximum duration of 10 Gyr in the case of the 2-system runs or until a convergent result is achieved in the case of the uniform medium runs.

The effects of ram pressure stripping are quantified by computing the mass of gas that remains gravitationally bound to the galaxy as a function of time. To determine which gas and dark matter particles are bound to the galaxy in any particular simulation output, we use the iterative method outlined in Tormen et al. (1998) and Hayashi et al. (2003). Starting from the distribution of particles that were bound at the previous simulation output (noting that all particles were bound initially), the potential, kinetic, and, in the case of the gas, the internal energies of each of the particles in the rest-frame of the galaxy are computed. We discard all particles for which the sum of the kinetic and internal energies exceeds the potential energy. The rest-frame of the bound structure is then recomputed, as are the energies of each particle, and any additional unbound particles are identified and discarded. This procedure is repeated until no further particles are identified as being unbound. Furthermore, it is implicit that once a gas particle has been lost due to stripping it cannot at a later time become gravitationally bound again (i.e., the mass of bound gas is necessarily a monotonically decreasing function of time). In this way, we are calculating a conservative lower limit to the mass of bound gas.

2.2 Numerical issues

There are a variety of numerical issues that could potentially affect the simulations and hamper the development of a physical model for ram pressure stripping. Perhaps of most concern is the effect of limited numerical resolution and, in the case of SPH simulations, the role of the artificial viscosity term, which itself is resolution-dependent. The artificial viscosity, which is necessary in order for SPH algorithms to capture shocks, acts like an excess pressure for the gas parti-

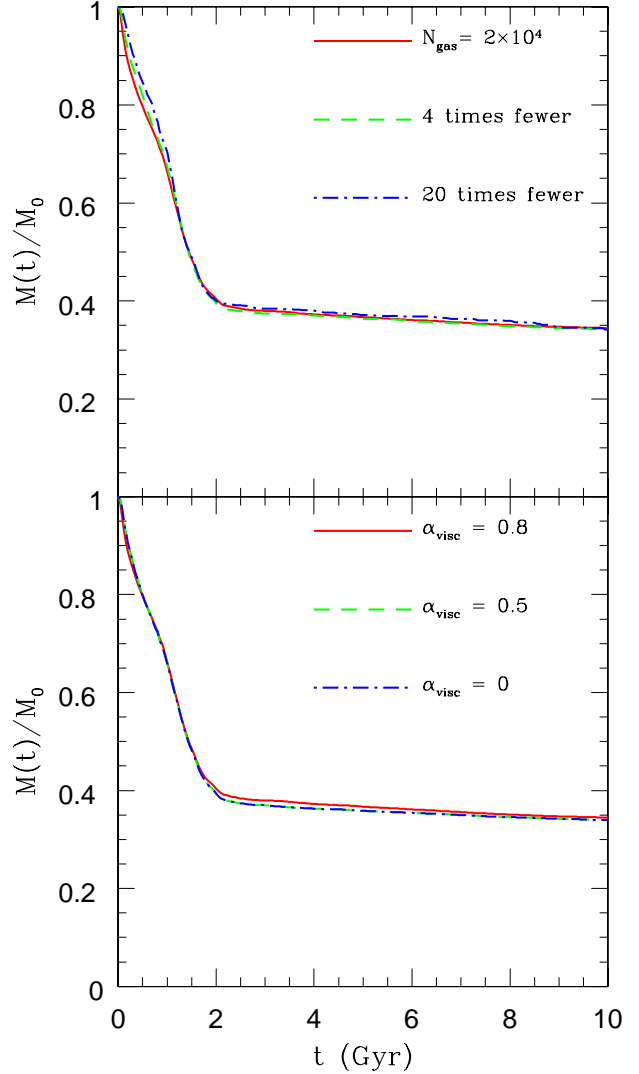


Figure 2. The effects of numerical resolution and artificial viscosity strength on the ram pressure stripping of the galaxy in the default 2-system run (see §3.3.1). Plotted is the ratio of gravitationally bound gas mass at time t to the initial mass of gas (at $t = 0$) versus time. In the top panel, we show the effect of raising the gas particle mass (i.e., lowering the particle number) from our default gas mass resolution of $m_{\text{gas}} = 2.82 \times 10^7 M_\odot$. In the bottom panel, we show the effect of lowering the SPH artificial viscosity parameter α_{visc} .

cles in their equation of motion and is therefore potentially relevant to our discussion of ram pressure stripping.

We have investigated the effects of numerical resolution and artificial viscosity in our default 2-system run (see §3.3.1 for a description of this run). The results are plotted in Figure 2. In the top panel, we show the effect of degrading the mass resolution of the gas particles (the mass resolution of the dark matter particles is the same for all these runs) on the ram pressure stripping of the galaxy. In the default case, there are 2×10^4 bound gas particles inside r_{200} of the galaxy initially. Reassuringly, we find that lowering the

number of particles does not significantly affect the resulting bound mass of gas as a function of time. This is the case even when the gas halo is represented initially by only 1000 particles. In fact, significant ($> 20\%$) differences appear only when the initial gas particle number in the galaxy is lowered to a few hundred (not shown). Note that the top panel of Fig. 2 implies that our results are not strongly sensitive to the artificial viscosity, since this is a resolution-dependent quantity.

The bottom panel of Fig. 2 adds further confidence that the results are robust. Here, we experiment with lowering the α_{visc} parameter, which controls the effective ‘strength’ of the artificial viscosity and is proportional to the excess pressure assigned to each gas particle in the equation of motion. Lowering the value of α_{visc} from the default value of 0.8 has no significant consequences for the resulting bound mass of gas. This is the case even when the artificial viscosity is set to zero².

We conclude that our ram pressure results are robust to our choice of resolution and artificial viscosity strength. It should be noted, however, that ram pressure is not the only mechanism by which gas can be stripped from galaxies as they orbit about groups and clusters. In particular, Kelvin-Helmholtz (KH) and Rayleigh-Taylor (RT) instabilities can potentially develop at the interface between the hot halo of the galaxy and the ICM and eventually completely disrupt or destroy the gaseous halo of the galaxy. It is known that SPH simulations tend to suppress such instabilities in the presence of large density gradients across the interface. This, in turn, will make the hot halo of a galaxy more resilient to stripping than it otherwise would have been. A good example of this can be found in Agertz et al. (2007), where a comparison between several Eulerian grid-based codes (which accurately follow the growth of these instabilities) and several Lagrangian SPH codes is performed for an idealised case where a ‘blob’ of gas moves through a uniform density medium. For example, their Fig. 4 shows that, for one particular case, the grid-based codes all predict complete disruption of the blob at $t \gtrsim \tau_{\text{KH}}$ (where τ_{KH} is the KH timescale, i.e., the time it takes KH instabilities to fully grow), whereas the SPH codes predict that the blob should remain intact.

With this in mind, one might conclude that SPH simulations such as ours will overestimate the survivability of the hot halo of a galaxy. However, it is important to note that Agertz et al. find that the grid-based and SPH-based codes agree with each other rather well for $t \lesssim \tau_{\text{KH}}$ (see also Appendix A of the present study). Following the approach of Mori & Burkert (2000) (see also Nulsen 1982; Murray et al. 1993; and Mayer et al. 2006), the Kelvin-Helmholtz timescale (including the stabilising effects of gravity) can be estimated as:

$$\begin{aligned} \tau_{\text{KH}} &= \frac{FM_0}{\dot{M}_{\text{KH}}} \\ &= 2.19 \times 10^9 \left(\frac{F}{0.1} \right) \left(\frac{M_0}{10^9 M_\odot} \right)^{1/7} \\ &\quad \times \left(\frac{n_{\text{ICM}}}{10^{-4} \text{ cm}^{-3}} \right)^{-1} \left(\frac{v_{\text{gal}}}{10^3 \text{ km s}^{-1}} \right)^{-1} \text{ yr} , \end{aligned} \quad (4)$$

where F is the baryon fraction of the galaxy, M_0 is the total mass of the galaxy within the radius down to which the galaxy has been stripped by ram pressure, n_{ICM} is the number density of hydrogen atoms in the ICM, and v_{orb} is the velocity of the galaxy with respect to the ICM.

For our default 2-system run (see §3.3.1), for example, we estimate from eqn. (4) that the Kelvin-Helmholtz timescale at pericentre is approximately 4.5 Gyr (i.e., which is comparable to the duration of our simulations). Since most of the orbital period of the galaxy is spent far from pericentre, the value of τ_{KH} will be substantially longer than this. Note also that the timescale associated with the growth of RT instabilities is comparable to or exceeds τ_{KH} . Therefore, we do not expect KH or RT instability stripping to have important consequences for the results or conclusions of this study. We also point out that eqn. (4) neglects the possibly important effects of radiative cooling, physical viscosity, magnetic fields, etc., all of which will tend to damp (and possibly halt) the growth of such instabilities in real cluster galaxies.

Finally, in order to dispel any lingering doubts that our adopted SPH approach is unable to treat ram pressure stripping accurately, we have made a direct comparison of the predictions of the Lagrangian SPH code GADGET-2 and the Eulerian AMR code FLASH for one of our uniform medium runs. This comparison is presented in Appendix A and shows that there is excellent quantitative agreement between the results of the two codes.

3 RESULTS

3.1 Analytic expectations

The study of ram pressure stripping of galaxies as they fall into groups and clusters dates back to the seminal paper of Gunn & Gott (1972). Using a static force argument, these authors derived a simple, physically-motivated condition for the instantaneous ram pressure stripping of a gaseous disk moving face-on through the ICM. The gas will be stripped if the ram pressure, P_{ram} , defined as $\rho_{\text{ICM}} v_{\text{orb}}^2$ (where ρ_{ICM} is the density of the ICM and v_{orb} is the speed of the galaxy with respect to the ICM), exceeds the gravitational restoring force per unit area on the disk, which they derive as $2\pi G \Sigma_* \Sigma_{\text{gas}}$ (where Σ_* and Σ_{gas} are the stellar and gaseous surface densities of the disk, respectively). We now seek to derive an analogous model for the ram pressure stripping of a spherically-symmetric gas distribution.

Since it is the least bound material, gas at the outer projected edge of the system will be stripped first (see the schematic diagram in Figure 3). Consider gas in a projected annulus between radii R and $R + dR$. The projected area of this annulus, dA , is $2\pi R dR$. Therefore, the force due to

² This may seem somewhat surprising at first glance since the galaxy is moving at a high velocity and therefore shock heating might be expected to be important (i.e., it could raise the entropy of the gas causing some of it to become unbound). However, as discussed in §3.1 (see also M07), both idealised and cosmological simulations show that shock heating of the gas halos of galaxies accreted by groups and clusters is unimportant. Most of the interaction energy is thermalised in the ICM of the main halo.

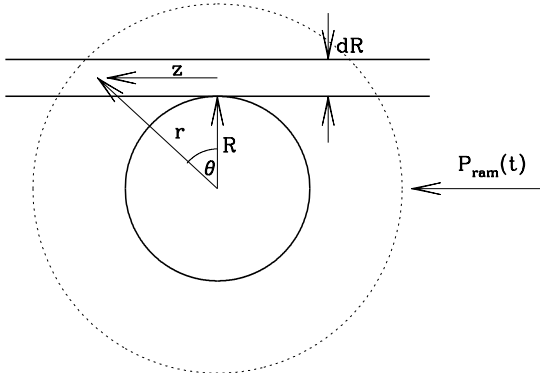


Figure 3. A schematic diagram of the ram pressure stripping of a spherically symmetric gas distribution. Here, the ram pressure force is directed from left to right and we consider the ratio of the ram pressure force to the gravitational restoring force per unit area for a projected annulus of width dR at the outer edge (radius R) of the gaseous halo of the galaxy.

ram pressure on this annulus is simply $F_{\text{ram}} = P_{\text{ram}} dA$. The annulus of gas will be displaced in the direction opposite to v_{orb} (which we will call the z direction) and will be stripped if the force due to the ram pressure exceeds the maximum gravitational restoring force in this direction. The maximum gravitational restoring force, F_{grav} , can be written approximately as $g_{\text{max}}(R) \Sigma_{\text{gas}}(R) dA$, where $g_{\text{max}}(R)$ is the maximum restoring acceleration in the z direction and $\Sigma_{\text{gas}}(R)$ is the projected surface density of the gas in the annulus. Therefore, the ram pressure stripping condition can be written as:

$$\rho_{\text{ICM}} v_{\text{orb}}^2 > g_{\text{max}}(R) \Sigma_{\text{gas}}(R). \quad (5)$$

If the gas density and total mass profiles of the galaxy can be represented by simple power laws, it is straightforward to evaluate the right-hand side of equation (5). In the case of a singular isothermal sphere, for example, where $\rho_{\text{gas}}(r) \propto r^{-2}$ and $M_{\text{gal}}(r) \propto r$ (where $M_{\text{gal}}(r)$ is the total mass within radius r), we find $g_{\text{max}}(R) = GM_{\text{gal}}(R)/(2R^2)$ and $\Sigma_{\text{gas}}(R) = \pi \rho_{\text{gas}}(R) R$. This leads to the following stripping condition

$$P_{\text{ram}}(t) > \frac{\pi}{2} \frac{GM_{\text{gal}}(R) \rho_{\text{gas}}(R)}{R}. \quad (6)$$

For more general gas density and total mass profiles, the condition for ram pressure stripping may be expressed as

$$P_{\text{ram}}(t) > \alpha \frac{GM_{\text{gal}}(R) \rho_{\text{gas}}(R)}{R}, \quad (7)$$

where α is a geometric constant of order unity which depends on the precise shape of the gas density and total mass profiles of the galaxy. We note that equation (7) is similar

to the analytic stripping conditions derived previously by Gisler (1976) and Sarazin (1979) (among others) for elliptical galaxies.

Equation (7) implies that all the gas beyond the 3D radius R_{strip} where the ram pressure exceeds the gravitational restoring force per unit area (which we will refer to as the stripping radius) will be stripped. By assumption, the properties of both the gas and dark matter within the stripping radius are unmodified by the stripping. The left-hand side of eqn. (7) makes it clear that the ram pressure is, in general, a function of time (i.e., for non-circular orbits).

Below, we use the idealised uniform medium runs to test this simple analytic model. However, before doing so it is worth briefly discussing some of the assumptions of this simple model and their validity. Firstly, the model neglects KH and RT instability stripping but, as we argued in §2.2, we do not expect this to be an important omission. Perhaps of more concern is that, by assuming that the properties of the system within the stripping radius do not change with time, the model implicitly neglects environmental effects such as tidal stripping and gravitational shock heating. In Appendix B, we show, using a simple argument, that one expects ram pressure stripping to be more efficient than tidal stripping for cases where the mass of the galaxy is less than about 10% of the mass of the group. In other words, for galaxies with masses of less than about 10% of the group mass, tidal stripping is not expected to substantially modify the structure of the galaxy within its stripping radius. Our 2-system runs involve only systems with mass ratios $\geq 10:1$.

The neglect of shock heating would naively appear to be a more serious omission, since the commonly-held picture of structure formation is that gas accreted by a massive system is shocked at the virial radius up to the virial temperature of the massive system. Thus, one might expect the hot gas halo of the galaxy to be quickly shock heated and become unbound. However, high resolution simulations (both cosmological and idealised) do not confirm this picture. In particular, if the material being accreted is in small dense “lumps” (e.g., low-mass virialised systems, as in the present case), it can penetrate all the way to the core of the massive system without being significantly shocked (e.g., Motl et al. 2004; Murray & Lin 2004; Poole et al. 2006; M07; Dekel & Birnboim 2007). In fact, most of the interaction energy is thermalised in the ambient medium of the more massive system (the ICM, in this case), while the accreted gas sinks to bottom of the potential well (see M07 for a detailed discussion). However, M07 found that the fraction of the total energy that is thermalised in the gas of the less massive system (the galaxy, in this case) increases almost linearly with the ratio of the mass of the less massive system to the total mass of both systems. Therefore, shock heating is expected to become important for cases where the mass of the galaxy is comparable to the mass of the group. Our 2-system runs, however, only involve galaxies with masses lower than 10% of the mass of the group.

3.2 Uniform medium runs

We now explore the ram pressure stripping of galaxies as they move through a uniform density gaseous medium. For the uniform medium, we select densities that are typical of the group/cluster environment. The temperature of the

medium is set such that its pressure equals that of the hot halo of the galaxy at its outer edge (i.e., the gaseous halo would be static if it were not moving with respect to the uniform medium). The galaxies are assigned velocities typical of systems orbiting in genuine groups and clusters (i.e., comparable to the circular velocity of the group or cluster).

In Fig. 4 we plot the bound mass of gas as a function of time for a small selection of the uniform medium runs we have performed and compare this with our proposed analytic model. We focus first on the $M(t)$ curves from the simulations (solid red curves). Firstly, the $M(t)$ curves in both panels asymptote to a particular value, as one would expect from the physical model proposed above where the ram pressure is effectively held constant with time but is low enough that not all of the gas should be stripped. In the bottom panel, where a galaxy is moved through media of two different densities but with velocities chosen such that the ram pressure is the same, the resulting $M(t)$ curves are very similar. This unambiguously demonstrates that the mass loss is indeed due to ram pressure stripping.

A comparison to the predictions of equation (7) (horizontal dotted lines) demonstrates that the asymptotic behaviour of the simulations is reproduced if $\alpha \approx 2$. (Note that this is very similar to the analytic estimate of $\pi/2$ derived in §3.1 for an isothermal sphere.) In fact, all the uniform medium runs we have performed yield a value of α close to 2. However, it is immediately apparent that the approximation of instantaneous stripping is not a particularly good one. For example, in the cases plotted in Fig. 4 it takes ~ 1 Gyr of stripping to reach a convergent value (i.e., to reach the 3D radius where the ram pressure equals the gravitational force per unit area). This “time delay” has been noted previously in studies of the stripping of cold disks (e.g., Roediger & Brüggen 2006; 2007) and is expected on physical grounds; the hot halo of the galaxy can only respond to changes in the local environment on a finite timescale. What is the relevant timescale? If the galaxy is moving subsonically, a natural choice might be the sound crossing time; i.e., the time it takes for a pressure wave to cross the galaxy’s hot halo. If the galaxy is moving supersonically, a better choice might be the time it takes a forward shock to propagate across the galaxy (e.g., Nittmann et al. 1982; Mori & Burkert 2000). (Although, as we noted above, shock heating of the hot gas of the galaxy is minimal in our simulations.) Alternatively, Roediger & Brüggen (2007) estimate and use the timescale required for the ram pressure to accelerate the gas to the galaxy’s escape velocity. We have experimented with including a time delay factor into the analytic model (how we do this is described below) that is set to either of these three timescales. In practice, we find that use of either of these timescales leads to very similar results. This is not too surprising. The similarity between the sound and shock crossing times is due to the fact that, in the rest frame of the group, the galaxy is typically orbiting at transonic velocities (i.e., Mach number ~ 1). The similarity between the sound crossing time and the time required to accelerate gas to the galaxy’s escape velocity is also not coincidental. Since the galaxy’s hot halo is in approximate hydrostatic equilibrium, the mean temperature of the gas will be close to the overall virial temperature of the galaxy (which is dominated by the mass in dark matter) and therefore the sound crossing time of the hot halo will be of order the dynamical time

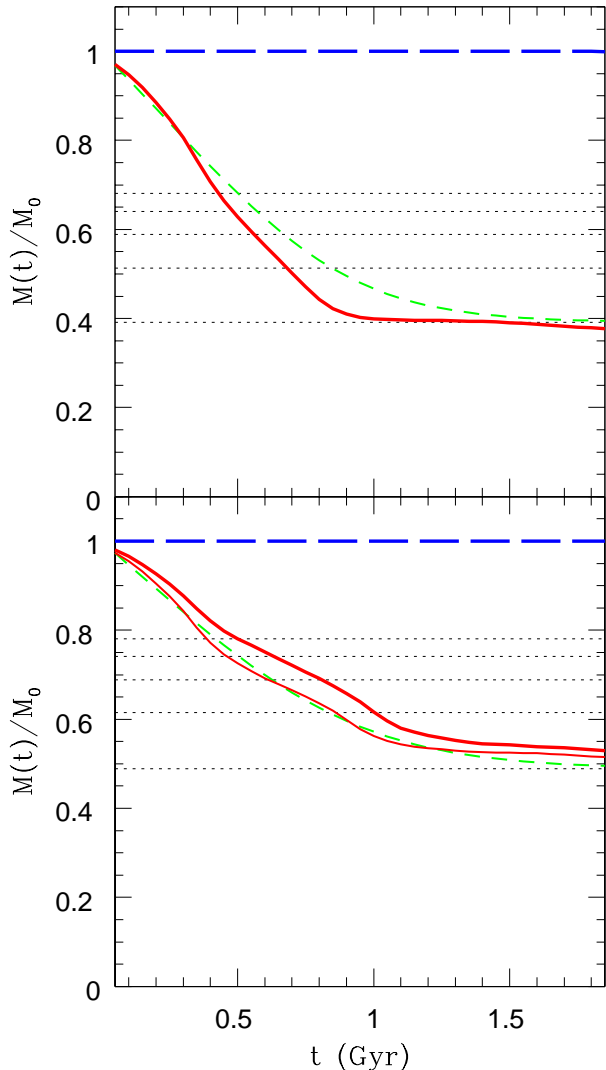


Figure 4. An example of ram pressure stripping in the uniform medium simulations. In the top panel, a galaxy of mass $M_{200} = 4 \times 10^{12} M_{\odot}$ is run through a uniform gaseous medium of density $100 f_b \rho_{\text{crit}}$ at a velocity of 1000 km s^{-1} . The solid red and dashed blue curves show the bound mass of gas and dark matter (respectively) in the simulation. In the bottom panel, the same galaxy is run through two different media: the thick red curve corresponds to the case where the background density is the same as in the top panel, but the velocity is 760 km s^{-1} , while the thin red curve corresponds to the case where the velocity is 1000 km s^{-1} but the density is a factor of $(1000/760)^2$ times lower than in the top panel. Thus, the ram pressure is the same for both cases in the bottom panel. In both the top and bottom panels the horizontal dotted lines correspond to the predictions of equation (7) for $\alpha = 2, 4, 6, 8, \text{ and } 10$ (bottom to top). The green dashed curve corresponds to equation (7) with $\alpha = 2$ but with a time delay factor that accounts for how long it takes the galaxy to respond to ram pressure stripping (i.e., approximately a sound crossing time), as discussed in the text.

of the galaxy. Consequently, if the force due to the ram pressure is of order the gravitational restoring force, as is the case for typical transonic velocities, the time it takes to accelerate the gas to the escape velocity will be comparable to the sound crossing time. Note, however, that if the galaxy's motion is highly supersonic (or if the gas is not in equilibrium) one might expect differences between the three timescales. The present study does not consider this regime and instead focuses on the more physically relevant transonic regime where all three timescales are similar. Below, we present results based on using the sound crossing time only.

Note that the simulation $M(t)$ curves plotted in Fig. 4 show that the mass loss proceeds with time more or less linearly until convergence is achieved. (This is generally true of the 2-system runs presented below, as well.) We therefore assume that the mass of gas stripped over some time interval Δt is just the total mass of stripped gas inferred from the instantaneous assumption (i.e., the total gas mass external to the stripping radius) scaled by the ratio $\Delta t/t_{\text{ram}}$, where t_{ram} is the characteristic timescale for ram pressure stripping (i.e., approximately the sound crossing time). For an appropriate comparison to the simulations, we set Δt to the adopted simulation output time interval of 50 Myr.

The sound crossing time of the gaseous halo at any particular time is calculated as:

$$t_{\text{sound}} = \int_0^R \frac{dr'}{c_s(r')} \quad (8)$$

where R is the maximum radial extent of the bound galactic gas and $c_s(r)$ is the local sound speed profile, which is given by $[\gamma P_{\text{gas}}(r)/\rho_{\text{gas}}(r)]^{1/2}$ with $\gamma = 5/3$. Note that for an isothermal gas this leads to the familiar relation $t_{\text{sound}} = R/c_s$.

In fact, the time it takes the gaseous halo to respond to changes in the local environment will only be comparable to the sound crossing time, not exactly equal to it. We therefore multiply this timescale by an adjustable coefficient β (which will be of order unity) when computing how much mass can be stripped over a time interval (i.e., $t_{\text{ram}} = \beta t_{\text{sound}}$).

The resulting model is plotted in Fig. 4. In this case α has been fixed to 2 to obtain agreement with the asymptotic $M(t)$ behaviour of the simulated galaxies. A value of $0.5 < \beta < 0.7$ yields good agreement with the rate of decline of the bound gas mass seen early on in the simulations (shown is the case corresponding to $\beta = 2/3$). It is worth bearing in mind that the analytic model uses only the *initial* radial profiles of the galaxy to compute the bound mass of gas as a function of time. The fact that the model matches the simulations and that the required values of α and β are of order unity is encouraging.

As a further test of the analytic model, in Fig. 5 we plot the ratio of ram pressure to the restoring force per unit area (assuming $\alpha = 2$) at the outer edge of the gaseous halo of the simulated galaxy examined in the top panel of Fig. 4, as a function of time. This plot clearly demonstrates that at early times the ram pressure exceeds the gravitational restoring force per unit area, which is why stripping occurs. As shown in the top panel of Fig. 4, stripping continues until $t \approx 0.8$ Gyr and then stops rather abruptly. With Fig. 5 we now clearly see the reason for this behaviour: the ram pressure no longer exceeds the restoring force per unit area at the

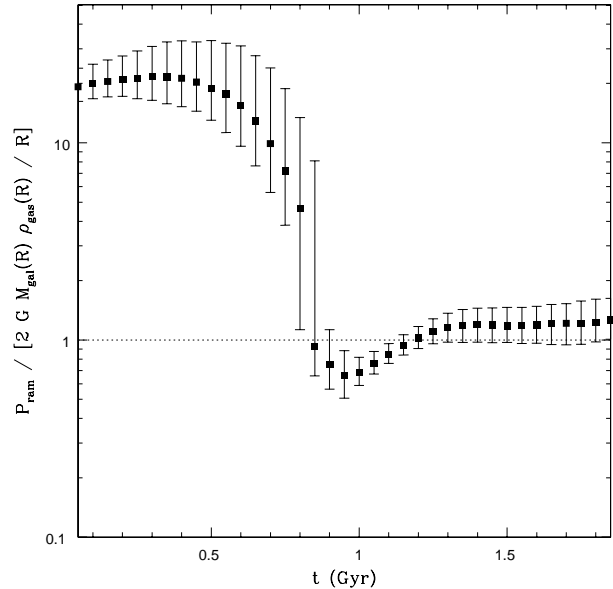


Figure 5. The ratio of ram pressure to gravitational restoring force per unit area (assuming $\alpha = 2$) at the outer edge of the gaseous halo of the galaxy plotted in the top panel of Fig. 4, as a function of time. The solid squares represent the median of the 500 outermost gravitationally bound gas particles while the error bars represent the 25th and 75th percentiles. After $t \approx 0.8$ the ram pressure and restoring force per unit area become comparable, which is why mass loss ceases after this time in Fig. 4.

outer edge of the bound halo after this time. In addition, we confirm that the maximum radial extent of the bound gas at $t > 0.8$ Gyr corresponds closely to the 3D radius where ram pressure equals the restoring force per unit area calculated from the *initial* gas distribution. This validates the basic assumptions of our analytic model, outlined in §3.1.

Having calibrated the analytic model against the uniform medium simulations (i.e., α and β are now fixed), we now proceed to see whether or not this simple physical model can also account for the mass loss in the more realistic 2-system runs.

3.3 2-system runs

3.3.1 The default 2-system run

The default 2-system run follows a massive galaxy with $M_{200} = 4 \times 10^{12} M_{\odot}$ falling into a moderate mass group of $M_{200} = 10^{14} M_{\odot}$ (implying a mass ratio of 25:1). As noted in §2, the concentration of these systems is set to match the mean mass-concentration of dark matter halos in the *Milennium Simulation*. The 2-system runs are initialised such that the virial radii (here defined as r_{200}) of the two systems are just barely touching. The adopted orbital parameters of the default run correspond to the most common orbit of infalling substructure measured in a large suite of cosmological simulations by Benson (2005; see his Fig. 2). Specifically, the initial relative radial velocity component, v_r , is set to $0.9v_c(r_{200})$ and the initial relative tangential component, v_t is set to $0.7v_c(r_{200})$, where $v_c(r_{200})$ is the circular velocity of the group at r_{200} . This corresponds to a total relative ve-

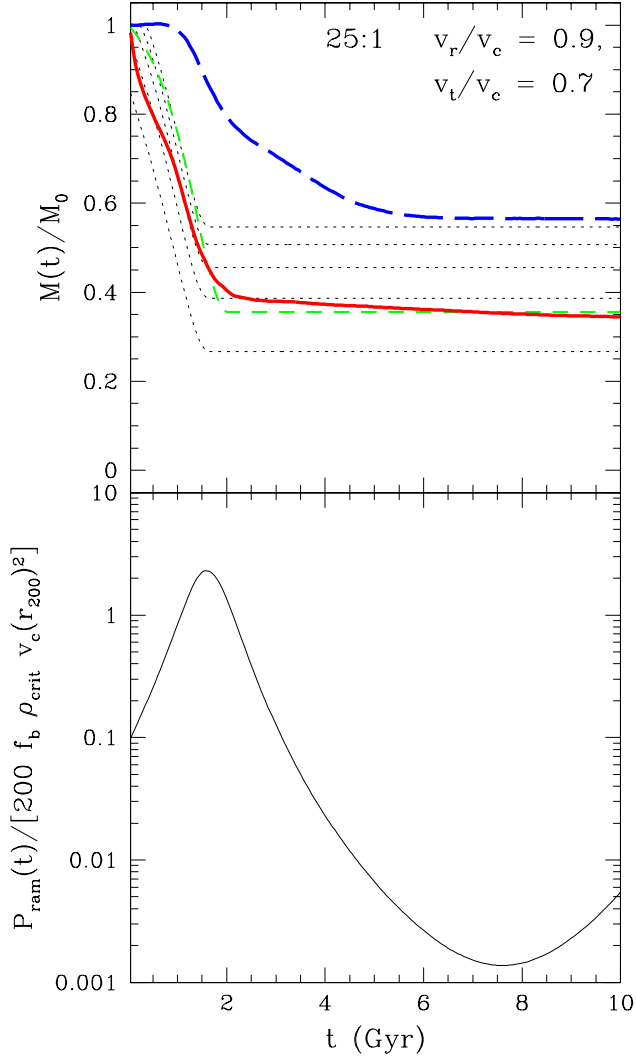


Figure 6. Ram pressure stripping in the default 2-system run. Top panel: the solid red and dashed blue curves show the bound mass of gas and dark matter, respectively, in the simulation. The green dashed curve corresponds to predictions of the analytic model (for $\alpha = 2$ and $\beta = 2/3$) where stripping occurs on approximately a sound crossing time. The dotted curves are the predictions of equation (7) with $\alpha = 2, 4, 6, 8$, and 10 (bottom to top) under the assumption of instantaneous stripping. Bottom panel: the ram pressure as a function of time as the galaxy orbits the group. The ram pressure has been normalised to the characteristic value of $\overline{\rho}_{\text{ICM}} v_c(r_{200})^2$. For this particular orbit, which corresponds to the most common orbit of infalling substructure in cosmological simulations, pericentric (apocentric) passage occurs at $t \approx 1.5$ Gyr ($t \approx 7.5$ Gyr).

locity of $\approx 1.1v_c(r_{200})$, which agrees well with the results of several other similar numerical studies (e.g., Tormen 1997; Vitvitska et al. 2002; Wang et al. 2005). In the following subsections, we experiment with varying the orbit, mass, and internal structure of the galaxy to test the generality of the analytic model.

As in the uniform medium runs, the analytic model is

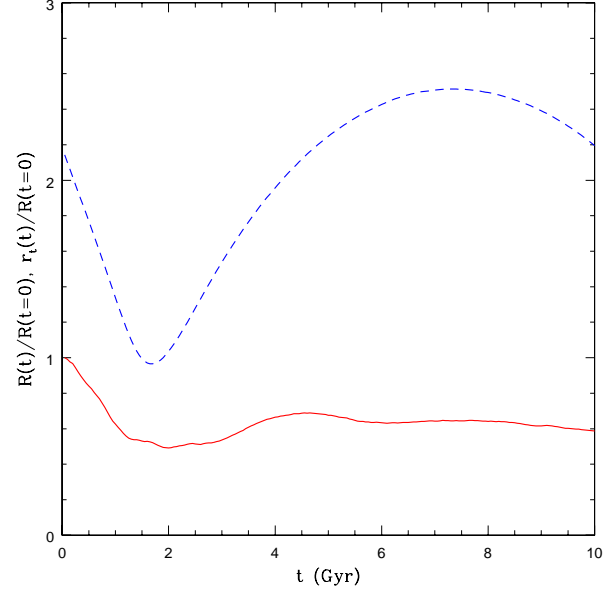


Figure 7. The evolution of the galaxy's tidal radius (dashed blue curve) and the radial extent of its bound gaseous halo (solid red curve) for the default 2-system run. The radial extent of the gas is defined here as the radius enclosing 90% of galaxy's bound hot halo. The tidal radius is larger than the bound hot gaseous halo by at least a factor of two at all times.

supplied with the initial conditions of the galaxy (i.e., its gas and dark matter radial profiles) and the magnitude of the ram pressure. In contrast to the uniform medium runs, however, the ram pressure is not constant with time. Using the orbit from the simulations, along with the density profile of the group, $P_{\text{ram}}(t)$ is calculated and passed to the analytic model. The analytic model can then predict $M(t)$ once the values of α and β have been selected.

The mass loss curves for the default 2-system run are plotted in the top panel of Fig. 6. Overall, the simple analytic model with $\alpha = 2$, $0.5 < \beta < 0.7$ (shown is $\beta = 2/3$) and $t_{\text{ram}} = \beta t_{\text{sound}}$ reproduces the mass loss seen in the default 2-system run very well. For example, both the simulations and the model show evidence for near convergence in $M(t)$ at $t \gtrsim 1.5$ Gyr, which corresponds to the (first) pericentric passage and, therefore, to the maximum ram pressure which the galaxy experiences along its orbit (see the bottom panel of Fig. 6).

The analytic model slightly underestimates the mass loss seen in the simulations at early times. This is a result of the fact that the hot halo of the galaxy is initially slightly over-pressurised with respect to the surrounding hot halo of the group. (Note that this was not the case for the uniform medium simulations plotted in Fig. 4.) This leads to some expansion of the outer gas which, in turn, makes it more susceptible to stripping. Since this effect is in general small and is an artifact of our idealised setup, we do not attempt to model it.

While the analytic model with a time delay factor matches the simulations well, an instantaneous stripping model with $\alpha \approx 4$ (represented by the second dotted curve from the bottom) also performs well. However, even if the

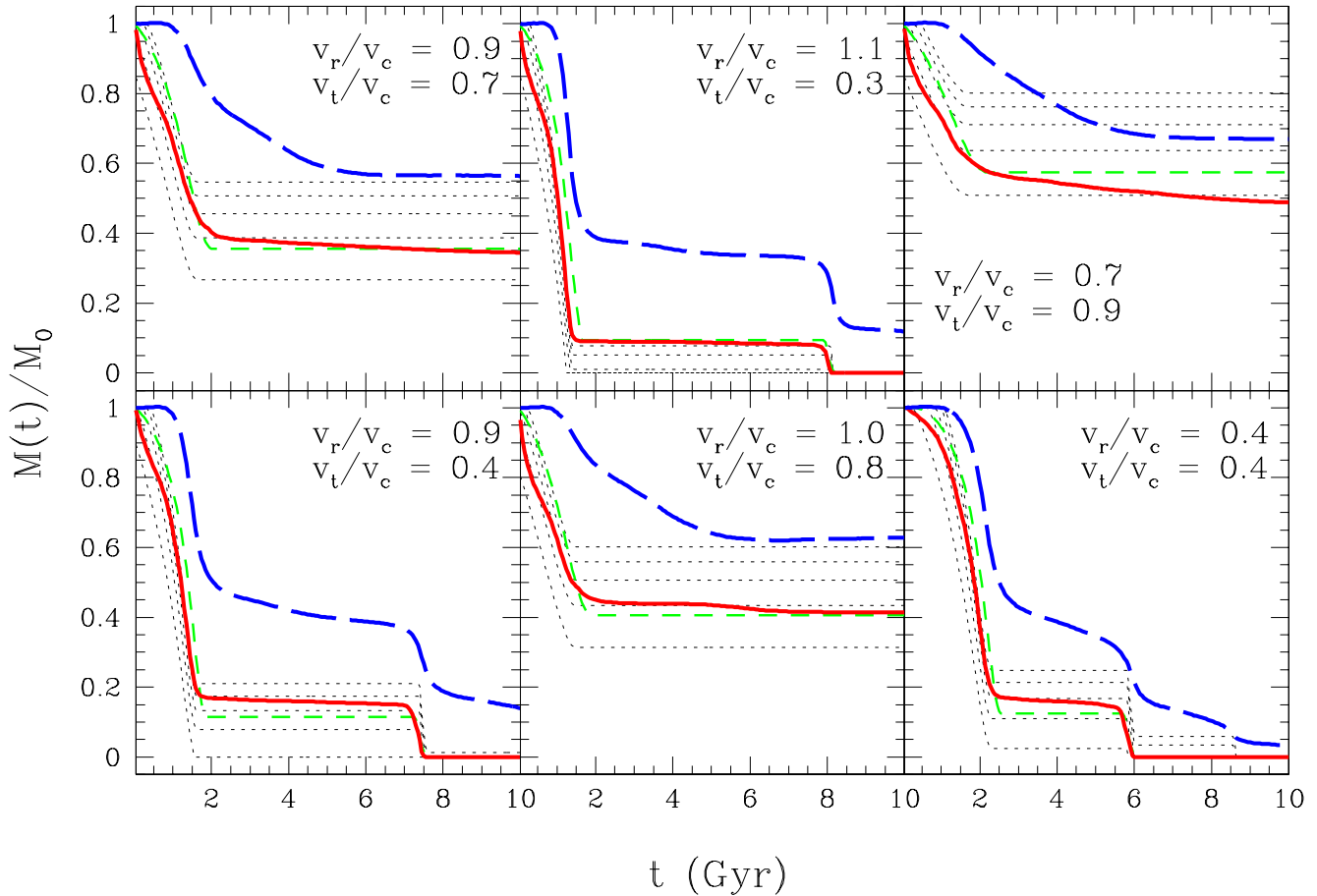


Figure 8. Ram pressure stripping as a function of initial orbital parameters. Shown are the mass loss curves of a galaxy with an initial mass $M_{200} = 4 \times 10^{12} M_{\odot}$ falling into a group with mass $M_{200} = 10^{14} M_{\odot}$. Each panel represents a different orbit, as described in the text. The line types have the same meanings as in Fig. 6.

agreement is reasonable, this model is without physical justification and should not be expected to apply in situations that differ significantly from those of the default run. Indeed, this is indicated by the results presented later in the paper (c.f. Fig. 8).

We also note that a significant fraction of the dark matter halo is also stripped, particularly near the first pericentric passage. This is not unexpected and is due to the tidal forces acting on the dark matter. We do not attempt to model the stripping of the dark matter, as there are already several published analytic studies which reproduce the dark matter stripping and tidal heating in simulations well (e.g., Taylor & Babul 2001; Benson et al. 2002). Instead, the analytic model proposed in §3.1 simply assumes that, within the stripping radius, the properties of the galaxy are unchanged from their initial state. Thus, the dark matter halo is assumed to maintain its initial NFW configuration within this radius. In Appendix B, we present a simple analytic argument that validates this assumption for systems where the mass of the galaxy is less than about 10% of the mass of the group. We have also directly computed the evolution of the tidal radius (r_t , defined in Binney & Tremaine 1987;

see also Appendix B) of the galaxy in the simulations as a function of time. In Fig. 7 we compare the tidal radius with the radial extent of the hot gaseous halo. The tidal radius shrinks at pericentre and then expands but at all times is safely larger than the gaseous halo by at least a factor of 2.

3.3.2 Varying the orbit of the galaxy

In Fig. 6 we examined the ram pressure stripping of a galaxy on the most common orbit seen in cosmological simulations. We now experiment with varying the initial orbital parameters. This will have the effect of changing both the shape and normalisation of $P_{\text{ram}}(t)$. We use Fig. 2 of Benson (2005) to select a range of cosmologically likely orbits; the initial velocity of some orbits is dominated by the radial component while others have nearly circular motions initially³. We plot the mass loss curves for six such orbits in Fig. 8.

³ In fact, unlike the other cases, the orbit with $v_r/v_c(r_{200}) = v_t/v_c(r_{200}) = 0.4$ is not a common one. We have simulated this atypical orbit just to see if the model breaks down for extreme cases.

The mass loss curves in Fig. 8 exhibit a variety of behaviours. Orbits that initially have a significant tangential component (and have a total velocity of $\sim v_c$) typically undergo only one pericentric passage over the course of 10 Gyr. Consequently, their associated $M(t)$ curves tend to show only one period of significant decline. Orbits that are predominantly radial, on the other hand, typically undergo two or more pericentric passages, with each successive passage bringing the galaxy closer to the centre of the group. In these cases we see two (or more) periods of significant decline in the bound mass of gas, as expected.

In spite of the widely varying orbits, the simple analytic model with $\alpha = 2$, $0.5 < \beta < 0.7$ (shown is $\beta = 2/3$), and $t_{\text{ram}} = \beta t_{\text{sound}}$ performs remarkably well in predicting the mass loss seen in the simulations. For all orbits and at all times the model predicts $M(t)$ to within $\approx 10\%$ accuracy.

Finally, it is interesting to note that if the standard (but unphysical) instantaneous ram pressure stripping model were adopted, the implication would be that α should vary as a function of the orbit. In particular, from Fig. 8, one would infer relatively low values of α ($\sim 2 - 5$) for more circular orbits and relatively high values of α ($\sim 6 - 10$) for more radial orbits. However, α is a geometric constant that is not expected to depend on the orbit. This consideration provided one of the original motivations for us to explore models where the stripping is not instantaneous. As we have demonstrated, a fixed value of $\alpha \approx 2$ works well for all orbits when one takes into account the finite time required for stripping.

3.3.3 Varying the mass of the galaxy

We now investigate variations in total mass of the galaxy. This will mainly have the effect of changing the gravitational restoring force (per unit area) of the galaxy at all radii by a constant factor. As indicated by Fig. 9, the analytic model matches the higher mass ratio interactions (lower galaxy masses) well at all times but does less well for the low mass ratio 10:1 at late times. In particular, the analytic model predicts that there ought to be no further stripping following first pericentric passage while the simulations show evidence for further stripping. What is the origin of this behaviour?

Inspection of the 10:1 simulation reveals that the gaseous halo of the galaxy undergoes significant expansion at late times while the analytic model uses the initial gas distribution (see Fig. 10). The expansion, in turn, makes the gas more susceptible to ram pressure stripping, and this accounts for the decline in the bound gas mass at late times. The physical reason for the expansion of the gaseous halo is as follows. At early times, the ram pressure exceeds the restoring force per unit area of the outer gas, which leads to stripping. This stripping proceeds until pericentric passage, when P_{ram} is largest. The remaining bound gaseous halo following pericentric passage is of higher mean density and pressure than the initial system, since all of the low density (less bound) material has been removed. Following pericentre, the galaxy moves out to large group-centric radii, where the pressure and density of the ICM are relatively low compared to pericentre. As a result, the gaseous halo of the galaxy becomes over-pressurised with respect to the local ICM and begins to expand. This effect is larger in the case of

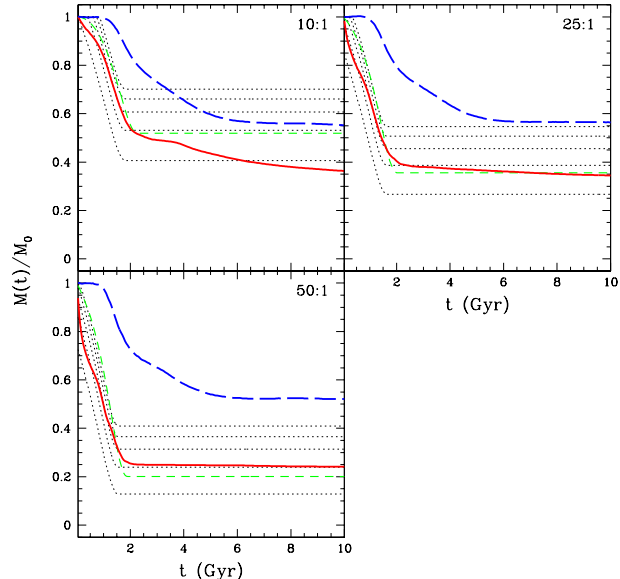


Figure 9. Ram pressure stripping as a function of galaxy mass. Shown are the mass loss curves for a galaxy of varying mass but with the same initial orbital parameters as in the default 2-system run. Each panel corresponds to galaxies with different total masses as is indicated by the mass ratio in the legend. (Note that the group mass is fixed at $M_{200} = 10^{14} M_{\odot}$ and the default case corresponds to a mass ratio of 25:1.) The line types have the same meanings as in Fig. 6.

more massive galaxies since they are more over-pressurised with respect to the ICM. The expansion proceeds until approximately apocentre is reached, at which point the galaxy begins to move back into denser and higher pressure regions of the group. (This effect is also responsible for the mild decline in bound gas mass for the highly tangential orbital case plotted in the top right-hand panel of Fig. 8.) It is important to note that this over-pressurisation effect is not a numerical artifact, it is a real effect that should be experienced by massive galaxies with orbits that have large energies and tangential components.

Modelling this effect may be possible with some effort. The expansion of the gaseous halo at late times is adiabatic, which greatly simplifies matters. One could therefore compute the radial properties of the gaseous halo as a function of time using the Lagrangian entropy distribution of the gas and assuming hydrostatic equilibrium with an outer boundary condition that the pressure must match that of the ambient ICM. However, this procedure is complicated by the fact that one must also know the distribution of the galaxy's dark matter halo out to the radius of maximum expansion. While the dark matter profile at small and intermediate radii is sufficiently similar to the initial distribution, this is not the case at very large radii. A proper treatment therefore requires that we factor in dark matter stripping and heating. This could potentially be achieved by combining our analytic ram pressure model with existing analytic models of dark matter stripping and heating (e.g., Taylor & Babul 2001; Benson et al. 2002). However, this is beyond the scope of the present study and we leave it for future work.

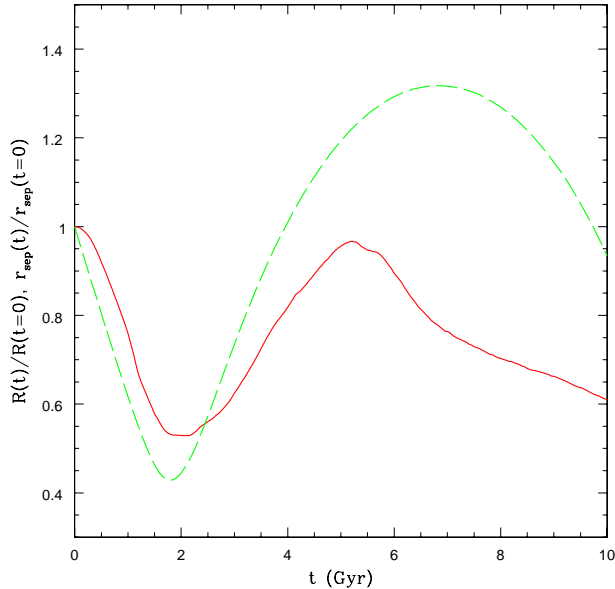


Figure 10. The evolution of the radial extent of bound gaseous halo (solid red curve) for the 10:1 2-system run plotted in Fig. 9. Also shown is the distance (r_{sep}) between the centres of the galaxy and group as a function of time. Following pericentric passage, the hot halo of the galaxy is over-pressurized compared to the ambient ICM and begins to expand. This expansion leads to further ram pressure stripping at late times.

Finally, we stress that the expansion effect just described is relevant to cases where both of the following are true: (1) the mass of the galaxy is greater than about 10% of the mass of the group; and (2) the orbit has an appreciable tangential component and a large enough energy such that apocentre occurs at large group radius⁴ (i.e., comparable to the group virial radius). However, we expect that both of these conditions are rarely fulfilled simultaneously in real systems, as massive satellites tend preferentially to fall into groups and clusters on nearly radial orbits (i.e., along filaments; see, e.g., Benson 2005).

3.3.4 Varying the concentration of the galaxy

Finally, we experiment with varying the internal structure of the galaxy (both its gas and dark matter) by varying its initial concentration parameter, c_{200} (equivalently, its scale radius, r_s). This will mainly have the effect of changing the shape of the radial profile of the restoring force (per unit area). This test is motivated by the fact that in cosmological simulations there is a large degree of intrinsic scatter in the concentration parameter for a system of fixed mass (e.g., Dolag et al. 2004; Neto et al. 2007). Note that changing the concentration can also mimic the addition of another mass component to the galaxy, such as a stellar component (which we have neglected to include explicitly).

⁴ For radial orbits, on the other hand, apocentre lies at smaller group radius and, as a result, the galaxy does not become over-pressurised with respect to the ICM. In these cases, the analytic model matches the mass loss in the simulations quite well.

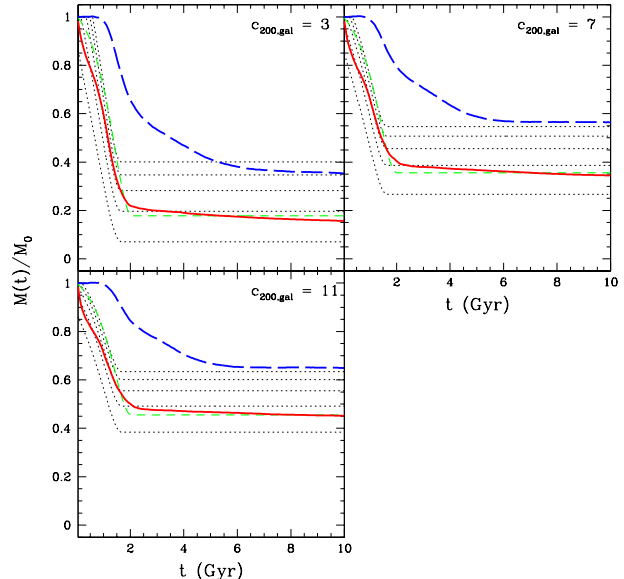


Figure 11. Ram pressure stripping as a function of galaxy internal structure. Shown are the mass loss curves of a galaxy with the same mass and orbit as the default run but with a varying concentration. Each panel corresponds to a different concentration parameter for the galaxy, with the default case corresponding to $c_{200} = 7$. The line types have the same meanings as in Fig. 6.

Fig. 11 shows that the concentration has a significant effect on the amount of gas that the galaxy is able to retain as it orbits about the group. As expected, as the concentration is increased so too is the bound mass of gas. As in the previous experiments, the simple analytic model with $\alpha = 2$, $0.5 < \beta < 0.7$ (shown is $\beta = 2/3$), and $t_{\text{ram}} = \beta t_{\text{sound}}$ matches the mass loss in the simulations very well.

4 SUMMARY AND DISCUSSION

Using a suite of carefully controlled 3D hydrodynamic simulations, we have investigated the ram pressure stripping of hot gas in the halos of galaxies as they fall into groups and clusters. We have proposed a physically simple analytic model that describes the stripping seen in the simulations remarkably well. This model is analogous to the original formulation of Gunn & Gott (1972), except that it is appropriate for the case of a spherical gas distribution (as opposed to a face-on disk) and takes into account that stripping is not instantaneous but occurs on approximately a sound crossing time. The only pieces of information that the model requires are the initial conditions of the orbiting galaxy (its gas and dark matter profiles), the density profile of the ICM and the orbit [the latter two are needed to calculate $P_{\text{ram}}(t)$]. The model contains two tunable coefficients that are of order unity. Fixing these coefficients to match the stripping in just one of our idealised uniform medium simulations (see §3.2) leads to excellent agreement with all our other simulations. With the exception of cases where the mass of the galaxy is greater than about 10% of the mass of the group and its orbit is highly non-radial, the analytic model reproduces the mass loss in the simulations to $\approx 10\%$ accuracy at

all times and for all the orbits, galaxy masses, and galaxy concentrations that we have explored. For cases where the mass of the galaxy exceeds 10% of the mass of the group, it will likely be necessary to factor in the effects of tidal stripping and gravitational shock heating, which are neglected by our model.

We re-iterate that the numerical simulations with which our analytic model has been calibrated have been demonstrated to be robust to the adopted resolution and artificial viscosity strength (see §2.2). Furthermore, as we have demonstrated that KH (and RT) instability stripping is expected to be unimportant, SPH codes should be fully capable of tackling the problem of hot halo gas stripping in galaxies orbiting in groups and clusters. A direct comparison between the results using the GADGET-2 and FLASH hydrodynamic codes for one of our runs (see Appendix A) confirms this conclusion.

The model we have derived has a number of potentially interesting applications, including modelling observed satellite galaxies and satellite galaxies in cosmological simulations. One application that we are currently pursuing is the incorporation of our ram pressure stripping model into a semi-analytic model of galaxy formation. As mentioned in §1, recent observations (Weinmann et al. 2006; Baldry et al. 2006) have revealed that current semi-analytic models predict satellite galaxies whose colours are too red compared to the observed systems. The implementation of ram pressure stripping in these models is unrealistically efficient since, by assumption, the hot halo of the satellite galaxy is instantly transferred to the more massive system as soon as the satellite galaxy enters the massive system's virial radius. In reality, the hot gaseous halo of the galaxy will remain intact for a while. For example, for the most common orbital parameters, we find that between 20%-40% of the initial hot halo of the galaxy can remain in place even after 10 Gyr of orbiting inside the group or cluster (see Fig. 9; note, however, that the quoted numbers could be sensitive to the adopted hot gas distribution of the galaxy). We note that these predictions are in qualitative agreement with recent *Chandra* X-ray observations of massive galaxies orbiting in hot clusters by Sun et al. (2007b), who find that most of the galaxies have detectable hot gaseous halos. Depending on the efficiency of feedback (e.g., from supernovae winds) in the semi-analytic models, radiative cooling of the remaining hot halo gas will replenish the cold gaseous component at the centre of the galaxy, which in turn will allow star formation to continue for some time. This will have the effect of making the colour of model satellite galaxies bluer and could resolve the discrepancy between semi-analytic models and observations (Font et al., in prep).

ACKNOWLEDGMENTS

The authors thank the referee for useful suggestions that improved the paper and they thank Simone Weinmann, Andrew Benson, Volker Springel and Frank van den Bosch for helpful discussions. IGM acknowledges support from a NSERC Postdoctoral Fellowship. CSF acknowledges a Royal Society Wolfson Research Merit Award. ASF acknowledges support from a PPARC Postdoctoral Fellowship. RGB acknowledges support from a PPARC Senior Fellowship. MLB

acknowledges support from a NSERC Discovery Grant. This work was supported in part by a PPARC rolling grant to Durham University. Some of the software used in this work was in part developed by the DOE-supported ASC / Alliance Center for Astrophysical Thermonuclear Flashes at the University of Chicago.

REFERENCES

- Abadi, M. G., Moore, B., & Bower, R. G. 1999, MNRAS, 308, 947
- Acreman, D. M., Stevens, I. R., Ponman, T. J., & Sakelliou, I. 2003, MNRAS, 341, 1333
- Agertz, O., et al. 2007, MNRAS, 380, 963
- Ascasibar, Y., & Markevitch, M. 2006, ApJ, 650, 102
- Baldry, I. K., Balogh, M. L., Bower, R. G., Glazebrook, K., Nichol, R. C., Bamford, S. P., & Budavari, T. 2006, MNRAS, 373, 469
- Balogh, M. L., Navarro, J. F., & Morris, S. L. 2000, ApJ, 540, 113
- Balogh, M. L., Baldry, I. K., Nichol, R., Miller, C., Bower, R., & Glazebrook, K. 2004, ApJL, 615, L101
- Benson, A. J. 2005, MNRAS, 358, 551
- Benson, A. J., Bower, R. G., Frenk, C. S., & White, S. D. M. 2000, MNRAS, 314, 557
- Benson, A. J., Lacey, C. G., Baugh, C. M., Cole, S., & Frenk, C. S. 2002, MNRAS, 333, 156
- Binney, J., & Tremaine, S. 1987, Princeton, NJ, Princeton University Press, 1987, 747, p. 233
- Cayatte, V., Kotanyi, C., Balkowski, C., & van Gorkom, J. H. 1994, AJ, 107, 1003
- Crowl, H. H., Kenney, J. D. P., van Gorkom, J. H., & Vollmer, B. 2005, AJ, 130, 65
- Dekel, A., & Birnboim, Y. 2007, ArXiv e-prints, 707, arXiv:0707.1214
- Dolag, K., Bartelmann, M., Perrotta, F., Baccigalupi, C., Moscardini, L., Meneghetti, M., & Tormen, G. 2004, A&A, 416, 853
- Dressler, A. 1980, ApJ, 236, 351
- Dressler, A. 1984, ARAA, 22, 185
- Eke, V. R., Navarro, J. F., & Steinmetz, M. 2001, ApJ, 554, 114
- Fryxell, B., et al. 2000, ApJS, 131, 273
- Gisler, G. R. 1976, A&A, 51, 137
- Goto, T., Yamauchi, C., Fujita, Y., Okamura, S., Sekiguchi, M., Smail, I., Bernardi, M., & Gomez, P. L. 2003, MNRAS, 346, 601
- Gómez, P. L., et al. 2003, ApJ, 584, 210
- Gunn, J. E., & Gott, J. R. I. 1972, ApJ, 176, 1
- Hayashi, E., Navarro, J. F., Taylor, J. E., Stadel, J., & Quinn, T. 2003, ApJ, 584, 541
- Hester, J. A. 2006, ApJ, 647, 910
- Hogg, D. W., et al. 2004, ApJL, 601, L29
- Jáchym, P., Palouš, J., Köppen, J., & Combes, F. 2007, A&A, 472, 5
- Kapferer, W., et al. 2007, A&A, 466, 813
- Kawata, D., & Mulchaey, J. S. 2007, ArXiv e-prints, 707, arXiv:0707.3814
- King, I. 1962, AJ, 67, 471
- Larson, R. B., Tinsley, B. M., & Caldwell, C. N. 1980, ApJ, 237, 692

Machacek, M., Jones, C., Forman, W. R., & Nulsen, P. 2006, *ApJ*, 644, 155

Mayer, L., Mastropietro, C., Wadsley, J., Stadel, J., & Moore, B. 2006, *MNRAS*, 369, 1021

McCarthy, I. G., et al. 2007, *MNRAS*, 376, 497 (M07)

McCarthy, I. G., Babul, A., Bower, R. G., & Balogh, M. L. 2007, *ArXiv e-prints*, 706, arXiv:0706.2768

Mori, M., & Burkert, A. 2000, *ApJ*, 538, 559

Motl, P. M., Burns, J. O., Loken, C., Norman, M. L., & Bryan, G. 2004, *ApJ*, 606, 635

Murray, S. D., & Lin, D. N. C. 2004, *ApJ*, 615, 586

Murray, S. D., White, S. D. M., Blondin, J. M., & Lin, D. N. C. 1993, *ApJ*, 407, 588

Navarro, J. F., Frenk, C. S., & White, S. D. M. 1996, *ApJ*, 462, 563

Navarro, J. F., Frenk, C. S., & White, S. D. M. 1997, *ApJ*, 490, 493

Neto, A. F., et al. 2007, *ArXiv e-prints*, 706, arXiv:0706.2919

Nittmann, J., Falle, S. A. E. G., & Gaskell, P. H. 1982, *MNRAS*, 201, 833

Nulsen, P. E. J. 1982, *MNRAS*, 198, 1007

Okamoto, T., & Nagashima, M. 2003, *ApJ*, 587, 500

Poggianti, B. M., Smail, I., Dressler, A., Couch, W. J., Barger, A. J., Butcher, H., Ellis, R. S., & Oemler, A. J. 1999, *ApJ*, 518, 576

Poole, G. B., Fardal, M. A., Babul, A., McCarthy, I. G., Quinn, T., & Wadsley, J. 2006, *MNRAS*, 373, 881

Quilis, V., Moore, B., & Bower, R. 2000, *Science*, 288, 1617

Roediger, E., & Brüggén, M. 2006, *MNRAS*, 369, 567

Roediger, E., & Brüggén, M. 2007, *MNRAS*, 380, 1399

Roediger, E., Brüggén, M., & Hoeft, M. 2006, *MNRAS*, 371, 609

Sakellou, I., Acreman, D. M., Hardcastle, M. J., Merrifield, M. R., Ponman, T. J., & Stevens, I. R. 2005, *MNRAS*, 360, 1069

Sarazin, C. L. 1979, *ApJ*, 20, L93

Sarazin, C. L. 1988, *Cambridge Astrophysics Series*, Cambridge: Cambridge University Press, 1988, pg. 212

Schindler, S., et al. 2005, *A&A*, 435, L25

Solanes, J. M., Manrique, A., García-Gómez, C., González-Casado, G., Giovanelli, R., & Haynes, M. P. 2001, *ApJ*, 548, 97

Springel, V. 2005, *MNRAS*, 364, 1105

Springel, V., & Hernquist, L. 2002, *MNRAS*, 333, 649

Springel, V., et al. 2005, *Nature*, 435, 629

Sun, M., & Vikhlinin, A. 2005, *ApJ*, 621, 718

Sun, M., Donahue, M., & Voit, G. M. 2007, *ArXiv e-prints*, 706, arXiv:0706.1220

Sun, M., Jones, C., Forman, W., Vikhlinin, A., Donahue, M., & Voit, M. 2007, *ApJ*, 657, 197

Takeda, H., Nulsen, P. E. J., & Fabian, A. C. 1984, *MNRAS*, 208, 261

Takizawa, M. 2005, *ApJ*, 629, 791

Taylor, J. E., & Babul, A. 2001, *ApJ*, 559, 716

Toniazzo, T., & Schindler, S. 2001, *MNRAS*, 325, 509

Tormen, G. 1997, *MNRAS*, 290, 411

Tormen, G., Diaferio, A., & Syer, D. 1998, *MNRAS*, 299, 728

Vikhlinin, A., Kravtsov, A., Forman, W., Jones, C., Markevitch, M., Murray, S. S., & Van Speybroeck, L. 2006, *ApJ*, 640, 691

Vitvitska, M., Klypin, A. A., Kravtsov, A. V., Wechsler, R. H., Primack, J. R., & Bullock, J. S. 2002, *ApJ*, 581, 799

Vollmer, B., Cayatte, V., Balkowski, C., & Duschl, W. J. 2001, *ApJ*, 561, 708

Vollmer, B., Braine, J., Combes, F., & Sofue, Y. 2005, *A&A*, 441, 473

Wang, H. Y., Jing, Y. P., Mao, S., & Kang, X. 2005, *MNRAS*, 364, 424

Weinmann, S. M., van den Bosch, F. C., Yang, X., Mo, H. J., Croton, D. J., & Moore, B. 2006, *MNRAS*, 372, 1161

APPENDIX A: COMPARISON OF RAM PRESSURE STRIPPING USING GADGET-2 AND FLASH

Here, we compare the results obtained using the Lagrangian SPH code GADGET-2 (Springel 2005) with those obtained using the Eulerian AMR code FLASH (Fryxell et al. 2000) for one of the uniform medium runs (specifically, the run presented in the top panel of Fig. 4).

The characteristics of the GADGET-2 simulation are given in §2.1 and §3.2 of the main text. For FLASH, we have tried three different versions of the same uniform medium run. In the first version, the galaxy is moved across a periodic box filled with a static background medium (as in the GADGET-2 simulation) and the computational volume is resolved with a fixed 256^3 base grid. This yields a spatial resolution comparable to that of the GADGET-2 run. In the second version, we take advantage of the AMR capability of FLASH, using a base grid of 64^3 cells and allowing up to two levels of refinement. This significantly speeds up the calculation. Finally, the third version is the same as the first version except that the galaxy is placed in the centre of the box and is assigned zero bulk velocity while the uniform background medium is assigned a velocity of -1000 km s^{-1} . Encouragingly, we find that all three versions of the FLASH run yield virtually identical results. Below, we compare only the results of the first version with the results of the GADGET-2 simulation.

For all of the GADGET-2 simulations presented in the main text, the bound mass of gas is determined by calculating the centre of mass of the galaxy, computing energies in this frame, throwing out unbound particles, recomputing the centre of mass, and so on until no further particles are identified as being unbound. Under this iterative scenario, once a particle is stripped it can never be re-accreted. The $M(t)$ curves are necessarily monotonically decreasing in this case. Unfortunately, it is not trivial to implement this type of algorithm for the FLASH simulation since it is not a Lagrangian code. Instead, it is simply assumed that all of the dark matter remains gravitationally bound (this is a good assumption, as indicated by the dashed blue curve in Fig. 4). We then use the dark matter halo to calculate the centre of mass of the galaxy and determine which of the gas cells in the box are gravitationally bound to this dark matter halo. Under this scenario, gas that was once stripped can potentially be re-accreted. Therefore, a direct comparison between the default GADGET-2 result and FLASH result should be treated with caution. Fortunately, however, it is

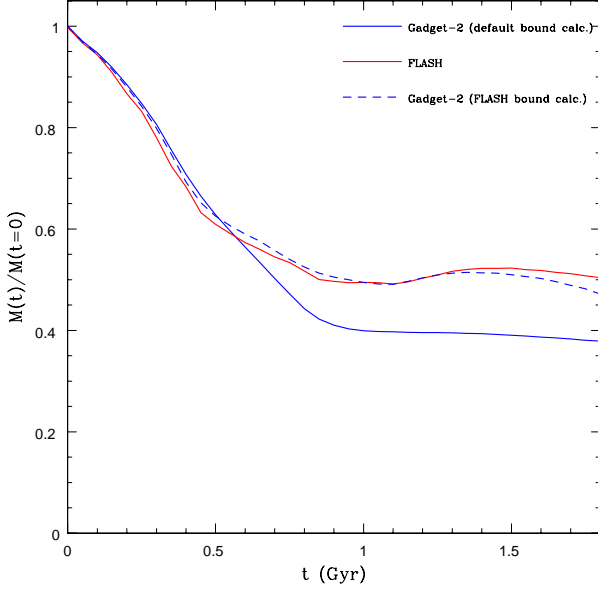


Figure 12. A comparison of the GADGET-2 and FLASH results for the bound mass of gas for the uniform medium run presented in the top panel of Fig. 4. The solid blue curve corresponds to applying the default iterative bound mass algorithm described at the end of §2.1 to the GADGET-2 run. The solid red curve are results of the FLASH code. The dashed blue curve corresponds to the case when we apply the same bound mass algorithm used for the FLASH run (see text) to the GADGET-2 run. This demonstrates that when the GADGET-2 and FLASH runs are treated on an equal footing the agreement between the two is excellent.

straightforward to apply the same simplified bound mass algorithm used for the FLASH run to the GADGET-2 run and we have done this.

In Fig. 12, we compare the bound mass of gas as a function of time for the GADGET-2 and FLASH runs. The plot demonstrates that when both runs are treated on an equal footing, using the same algorithm for computing the bound mass of gas, the agreement between them is superb.

APPENDIX B: THE IMPORTANCE OF TIDAL STRIPPING

Here, we present a simple argument that demonstrates that tidal stripping should only be relevant for cases where the mass of the galaxy exceeds $\sim 10\%$ of the mass of the group.

The tidal radius, r_t , of a galaxy can be expressed as

$$\frac{r_t}{R} = \left(\frac{M_{\text{gal}}(r_t)}{M_{\text{grp}}(R)(3 - d \ln M_{\text{grp}}/d \ln R)} \right)^{1/3}, \quad (9)$$

where R is 3D group-centric radius of the galaxy, $M_{\text{gal}}(r)$ is the total mass of the galaxy within radius r , and $M_{\text{grp}}(R)$ is the total mass of the group within radius R (e.g., King 1962).

The above equation can be re-written in terms of the mean density of the galaxy within r_t and the mean density of the group within R :

$$\overline{\rho_{\text{gal}}}(r_t) = \left(3 - \frac{d \ln M_{\text{grp}}}{d \ln R} \right) \overline{\rho_{\text{grp}}}(R). \quad (10)$$

For simplicity, we will now assume that both systems can be approximated as isothermal spheres. In this case, the condition for tidal stripping is simply

$$\overline{\rho_{\text{gal}}}(r_t) < 2 \overline{\rho_{\text{grp}}}(R). \quad (11)$$

We now seek to express the ram pressure stripping condition in terms of $\overline{\rho_{\text{gal}}}(r_t)$ and $\overline{\rho_{\text{grp}}}(R)$.

Assuming for both the galaxy and the group that the gas density traces the total density and that both have the same baryon fraction, eqn. (7) can be re-written as

$$\rho_{\text{grp}}(R) v_{\text{orb}}^2 > \alpha \rho_{\text{gal}}(r) v_{\text{c,gal}}^2(r). \quad (12)$$

Rearranging, we obtain

$$\rho_{\text{gal}}(r) < \frac{1}{\alpha} \left(\frac{v_{\text{orb}}}{v_{\text{c,gal}}} \right)^2 \rho_{\text{grp}}(R). \quad (13)$$

If both the galaxy and group have the same power law density profiles, then

$$\rho_{\text{gal}}(r) = k \overline{\rho_{\text{gal}}}(r) \quad (14)$$

$$\rho_{\text{grp}}(r) = k \overline{\rho_{\text{grp}}}(r)$$

for some k .

Therefore, the ram pressure stripping condition is given by

$$\overline{\rho_{\text{gal}}}(r) < \frac{1}{\alpha} \left(\frac{v_{\text{orb}}}{v_{\text{c,gal}}} \right)^2 \overline{\rho_{\text{grp}}}(R), \quad (15)$$

which is similar to the tidal stripping condition (eqn. 11) except that the right-hand side is larger by a factor F :

$$F = \frac{1}{2\alpha} \left(\frac{v_{\text{orb}}}{v_{\text{c,gal}}} \right)^2. \quad (16)$$

Typically, $v_{\text{orb}} \sim v_{\text{c,grp}}$ (where $v_{\text{c,grp}}$ is the circular of the group) and assuming $\alpha = 2$ the factor F can be expressed as

$$F \sim \frac{1}{4} \left(\frac{v_{\text{c,grp}}}{v_{\text{c,gal}}} \right)^2. \quad (17)$$

Since $v_c \propto M^{1/3}$ for cosmological halos, eqn. (17) can be re-written as

$$F \sim \frac{1}{4} \left(\frac{M_{\text{grp}}}{M_{\text{gal}}} \right)^{2/3}. \quad (18)$$

Tidal stripping is therefore only expected to become more important than ram pressure stripping (i.e., $F \gtrsim 1$) in cases where $M_{\text{gal}}/M_{\text{grp}} \gtrsim 1/8$.

This paper has been typeset from a \LaTeX file prepared by the author.